Transient Kinetics in the Oxidation of Carbon Monoxide Over a Silver Catalyst

by Masayoshi Kobayashi*, Hiroshi Takegami,**
Toshikazu Mori and* Nobuo Takahashi*

(Received April 30, 1983)

Abstract

The oxidation of carbon monoxide by nitrous oxide and oxygen over a silver catalyst at 20 C is analysed by both the Hougen-Watson procedure and the transient response method. The rival models derived from the Hougen-Watson procedure are not available to explain the transient response curves of N_2 and CO_2 caused by the concentration jump of CO and N_2O. A sound mechanism derived from the view based on the experimental transient behavior is visualized, and the kinetic parameters in all elementary steps in the reaction sequence are calculated as several parameter sets. From those rival parameter sets the best one is separately determined for the two CO oxdiations with N_2O and O_2, even though the two reactions contain some overlapped elementary steps, supporting the experimental finding on the heterogenity of silver surface. The best parameter set obtained for the respective reaction consistently explained all transient behavior.

1. Introduction

Bare silver surface reduced with hydrogen is fairly active for the adsorption of gaseous oxygen and the decomposition of nitrous oxide, forming the irreversible adsorption of oxygen.[1] Our previous work[2] has demonstrated that N_2O is directly decomposed on the bare silver surface. It may thus reasonably be visualized that the adsorption of gaseous oxygen on the active site will first form diatomic oxygen followed by successive dissociation to monoatomic oxygen, where-as in the decomposition of N_2O the reverse reaction will progress. Carbon mono-xide then attacks these two different oxygen species, when the oxidation of carbon monoxide is carried out on this oxidized surface. Both the oxidation of CO by O_2 and N_2O have some overlapping elementary steps such as dissociation or recombination of adsorbed oxygen species, surface reaction and desorption of carbon dioxide. Our interest is in whether the rate constants of such overlapped steps in the N_2O-CO reaction can be used in common for the O_2-CO reaction. If they are exchangable between both reactions, then the number of unknown kinetic parameters to be estimated by a parameter optimization technique is signi-ficantly reduced. Furthermore, simulating both reactions by using a computer, it is easy to confirm the validity of the estimated parameters. The two reactions

* Department of Industrial Chemistry, Kitami Institute of Technology, 090 Kitami, Hokkaido, Japn.

** Nihon Zeon Co.

thus can typically be employed to analyse the kinetic structure of reaction.

In the present study, for those two actual reactions, a discrimination of rival kinetic models derived from the conventional procedure is attempted by using the differences between the mode of transient response curves, which are calculated by a computer simulation technique. The calculated curves then refer to actual transient response curves to confirm the degree of fitting to the mode of the experimental curves.

Secondly, the most suitable reaction structure is proposed, based on the transient experimental data. The best parameter-sets for the rate constants of elementary steps in the reaction sequence of two reactions are calculated by the ordinary parameter optimization technique, Marquardt procedure. The rival parameter-sets in both reactions are also differentiated by referring to many experimental transient response curves. Finally, the best of the proposed parameter-sets for the two reactions will be determined.

2. Rival Models from the Hougen-Watson Procedure

In both the N_2O-CO and the O_2-CO reactions, the rate of CO_2 formation at steady state is not of first order with respect to the concentration of carbon monoxide, oxygen or nitrous oxide as shown in Figs. 1 and 2. For interpreting these rate data, a large number of possible models will be proposed. Of those models, three models for the N_2O-CO reaction and two models for the O_2-CO reaction, based on a Langmuir-Hinshelwood type and an Eley-Rideal type, may typically be proposed as presented in Table 1 by two groups Models 1–3 and 4–5 respectively. The equations (each of which corresponds to a model number in Table 1) are linearized, and the steady state rates calculated at various partial
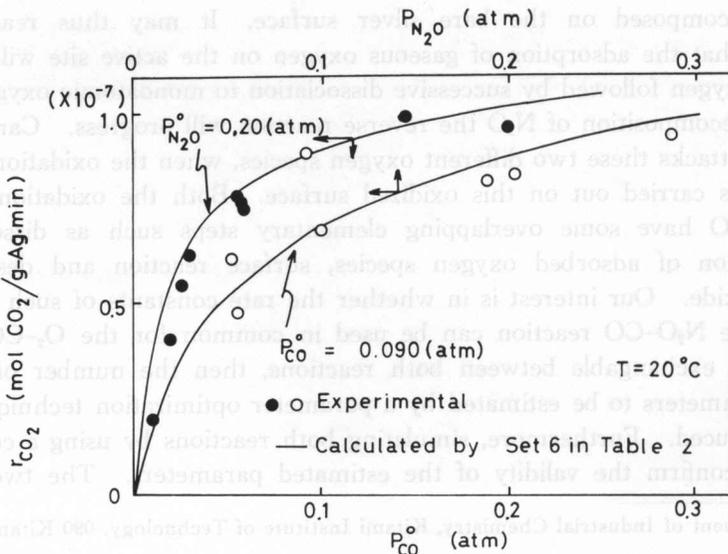

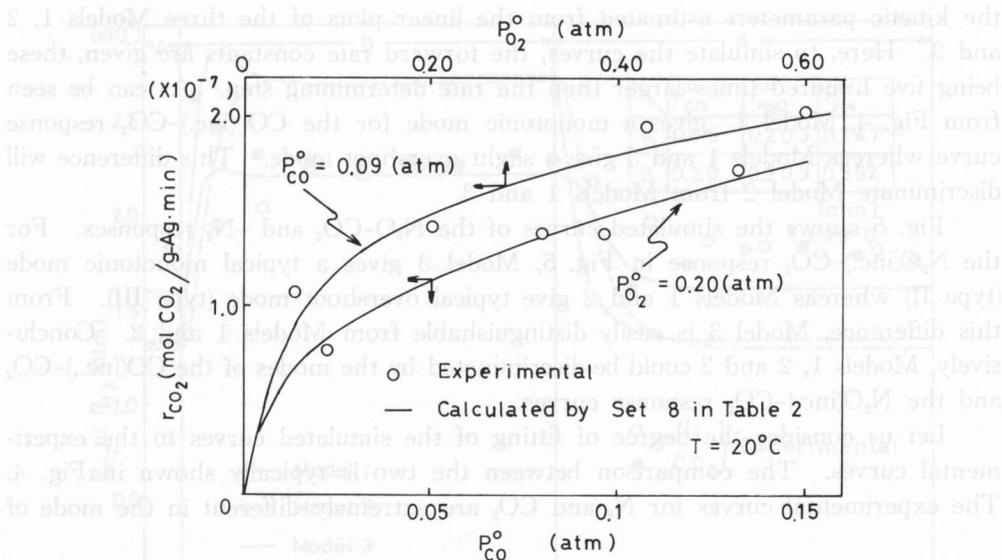**Fig. 1.** Plots of r_{CO_2} vs. P_{CO} and P_{N_2O}.

Fig. 2. Plots os of r_{CO_2} vs. P_{CO} and P_{O_2}.

Table 1. Kinetic Models for the N_2O–CO and the O_2–CO Reactions.

	Models	$10^6 \times k$ (mol/g. min.)	K_{CO} (atm^{-1})	K_{N_2O} (atm^{-1})	K_{O_2} (atm^{-1})
(1)	$\dfrac{kK_{CO}K_{N_2O}P_{CO}P_{N_2O}}{(1+K_{CO}P_{CO}+K_{N_2O}P_{N_2O})^2}$	0.539	24.3	13.9	—
(2)	$\dfrac{kK_{CO}P_{CO}P_{N_2O}}{1+K_{CO}P_{CO}+K_{N_2O}P_{N_2O}}$	1.82 atm^{-1}	210	110	—
(3)	$\dfrac{kK_{N_2O}P_{CO}P_{N_2O}}{1+K_{CO}P_{CO}+K_{N_2O}P_{N_2O}}$	1.82 atm^{-1}	210	110	—
(4)	$\dfrac{kK_{CO}K_{O_2}P_{CO}P_{O_2}}{(1+K_{CO}P_{CO}+K_{O_2}P_{O_2})^2}$	1.36	14.8	—	6.12
(5)	$\dfrac{kK_{O_2}^{1/2}P_{CO}P_{O_2}^{1/2}}{1+K_{CO}P_{CO}+K_{O_2}^{1/2}P_{O_2}^{1/2}}$	4.46 atm^{-1}	186.3	—	520.9

pressures of CO, N_2O and O_2 are compared with the five models. All the models are found to yield the same degree of fitting to the steady state rate data, indicating the difficulty in discriminating them, as can be seen in Fig. 3.

The mode of transient response curves of products caused by the concentration jump of reactants at the inlet of the reactor is significantly affected by reaction model.[3] This can conveniently be used to discriminate among the presented models. On the N_2O–CO reaction, Fig. 4 represents the simulated transient response curves of CO_2 or N_2 caused by the concentration jump of CO, using

the kinetic parameters estimated from the linear plots of the three Models 1, 2 and 3.   Here, to simulate the curves, the forward rate constants are given, these being five hundred times larger than the rate determining step.   As can be seen from Fig. 4, Model 2   gives a monotonic mode for the CO (inc.)-CO_2 response curve whereas Models 1 and 3 give a slight overshoot mode.   This difference will discriminate Model 2 from Models 1 and 3.

Fig. 5 shows the simulated curves of the N_2O-CO_2 and -N_2 responses.   For the N_2O(inc.)-CO_2 response in Fig. 5, Model 3 gives a typical monotonic mode (type II) whereas Models 1 and 2 give typical overshoot mode (type III).   From this difference, Model 3 is easily distinguishable from Models 1 and 2.   Conclusively, Models 1, 2 and 3 could be discriminated by the modes of the CO(inc.,)-CO_2 and the N_2O(inc.)-CO_2 response curves.

Let us consider the degree of fitting of the simulated curves to the experimental curves.   The comparison between the two is typically shown in Fig. 4. The experimental curves for N_2 and CO_2 are extremely different in the mode of
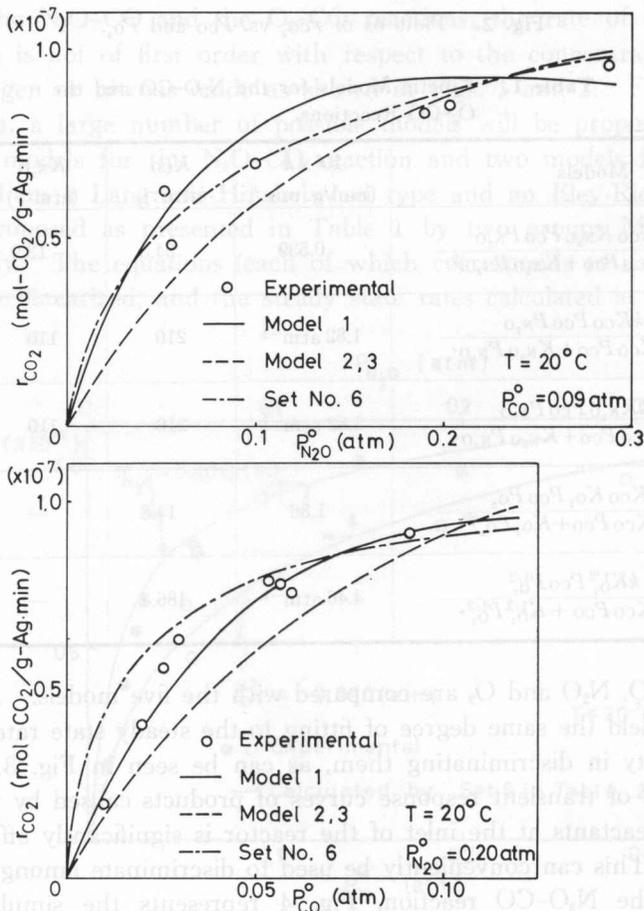

Fig. 3.   Steady state rate as function of P_{N_2O} and P_{CO} comparing between models.
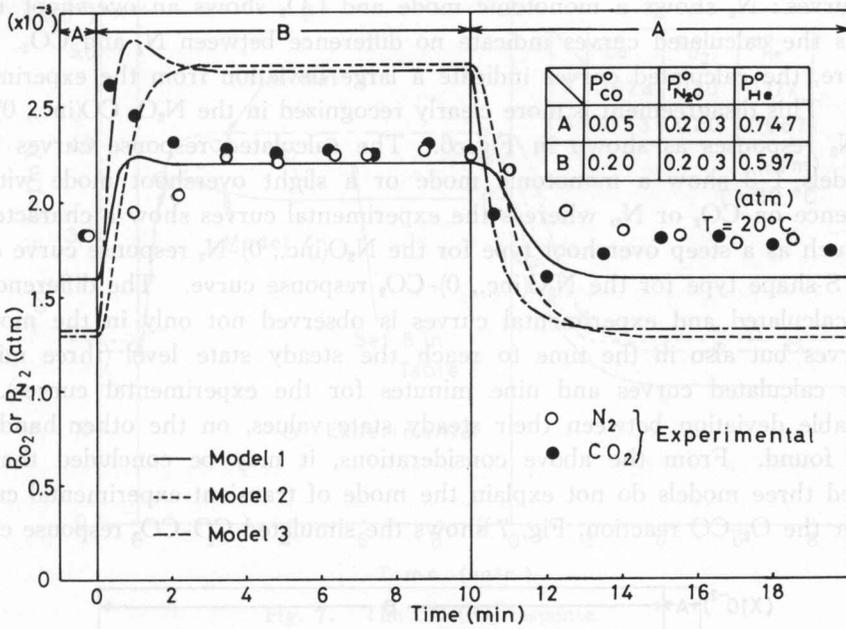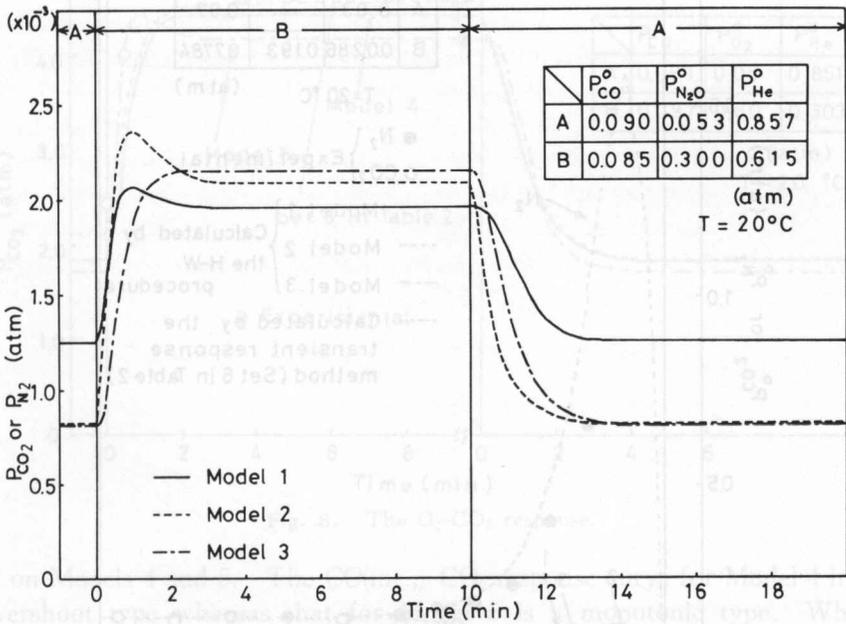
Fig. 4. The CO–CO₂ and –N₂ responses.

Fig. 5. The N₂O–CO₂ and –N₂ responses.

their curves : N_2 shows a monotonic mode and CO_2 shows an overshoot mode, whereas the calculated curves indicate no difference between N_2 and CO_2. Furthermore, the calculated curves indicate a large deviation from the experimental curves. This disagreement is more clearly recognized in the N_2O, CO(inc., 0)–CO_2 and –N_2 responses as shown in Fig. 6. The calculated response curves based on Models 1–3 show a monotonic mode or a slight overshoot mode with no dependence on CO_2 or N_2, whereas the experimental curves show a characteristic mode such as a steep overshoot type for the N_2O(inc., 0)–N_2 response curve and a typical S-shape type for the N_2O(inc., 0)–CO_2 response curve. The difference between calculated and experimental curves is observed not only in the mode of the curves but also in the time to reach the steady state level (three minutes for the calculated curves and nine minutes for the experimental curves). An appreciable deviation between their steady state values, on the other hand, can not be found. From the above considerations, it may be concluded that the proposed three models do not explain the mode of transient experimental curves.

For the O_2–CO reaction, Fig. 7 shows the simulated CO–CO_2 response curves
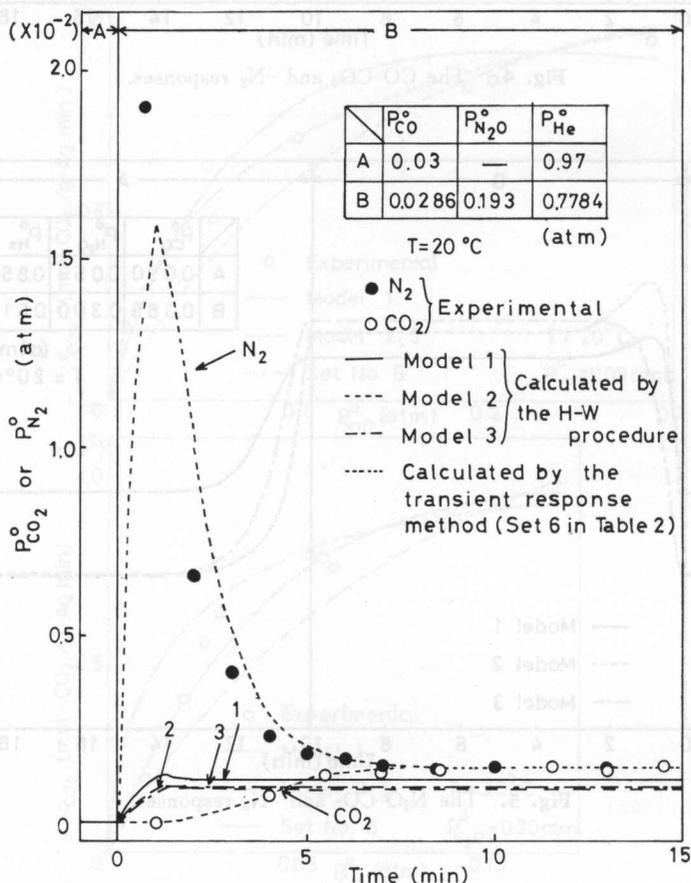

Fig. 6. The N_2O (inc., 0)–CO_2 and –N_2 responses on the reduced surface.
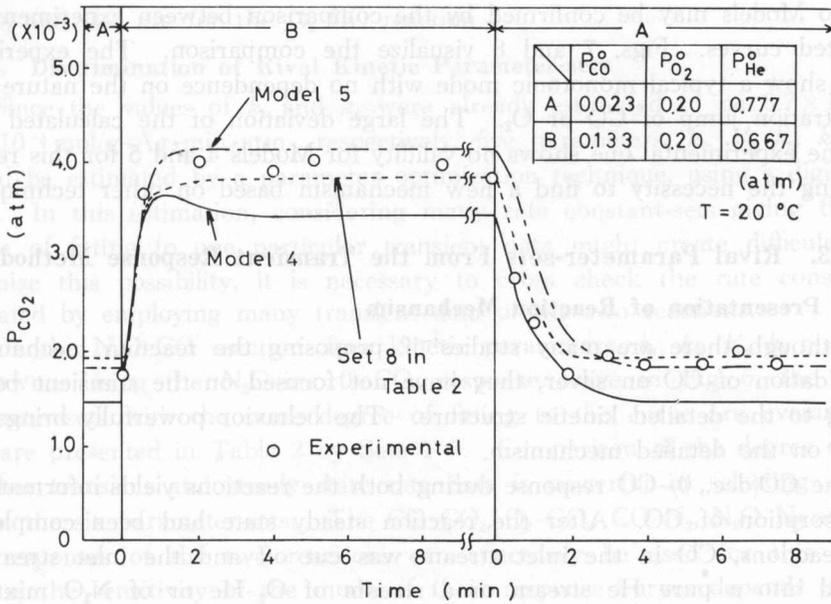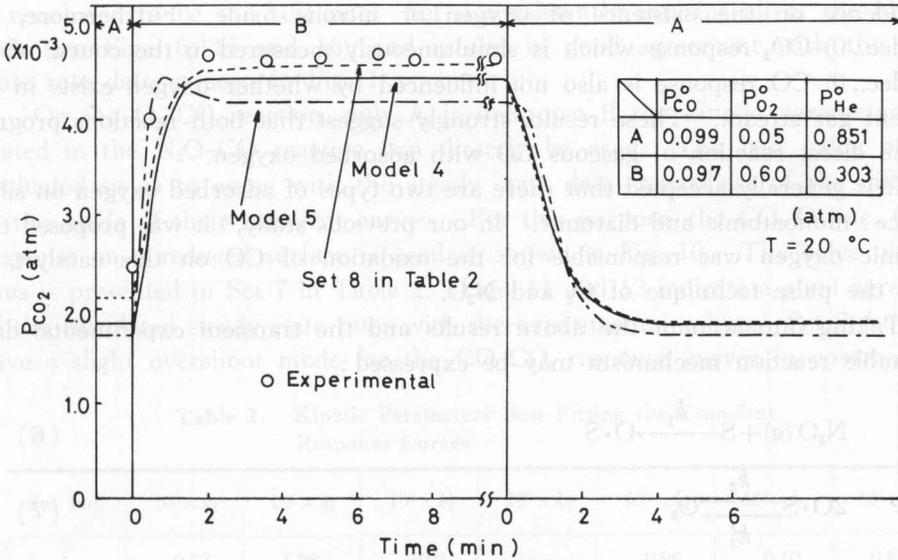
Fig. 7.   The CO–CO₂ response.

Fig. 8.   The O₂–CO₂ response.

based on Models 4 and 5.   The CO(inc.,)–CO_2 response curve for Model 4 indicates an overshoot type whereas that for Model 5 is a monotonic type.   When the O_2–CO_2 response, on the other hand, is carried out, Model 4 indicates a monotonic type and Model 5 indicates an overshoot type as shown in Fig. 8.   From these results, Models 4 and 5 can easily be differentiated by the mode of transient response curves in the concentration jump of CO or O_2.   Here, the validity of

the two Models may be confirmed by the comparison between experimental and calculated curves. Figs. 7 and 8 visualize the comparison. The experimental curves show a typical monotonic mode with no dependence on the nature of the concentration jump of CO or O_2. The large deviation of the calculated curves from the experimental one shows no validity for Models 4 and 5 for this reaction, indicating the necessity to find a new mechanism based on other techniques.

3. Rival Parameter-sets From the Transient Response Method

3-1. Presentation of Reaction Mechansim

Although there are many studies[4~11] proposing the reaction mechanism in the oxidation of CO on silver, they have not focused on the transient behavior relating to the detailed kinetic structure. The behavior powerfully brings to us a view on the detailed mechanism.

The CO(dec., 0)-CO response during both the reactions yields information for the adsorption of CO. After the reaction steady state had been completed in both reactions, CO in the inlet stream was cut off and the inlet stream was changed into a pure He stream or a stream of O_2–He or of N_2O mixture in a stepwise fashion. The CO (dec., 0)-CO response was separately followed in the individual run. All the responses responded to zero instantaneously with no dependence on the existence of oxygen or nitrous oxide. Furthermore, the CO (dec., 0)-CO_2 response which is simultaneously measured in the course of the CO (dec., 0)-CO response is also not influenced by whether oxygen exists in the ambient gas stream. These results strongly suggest that both reactions progress by the direct reaction of gaseous CO with adsorbed oxygen.

It is generally accepted that there are two types of adsorbed oxygen on silver surface : monoatomic and diatomic. In our previous study,[2] it was proposed that diatomic oxygen was responsible for the oxidation of CO on this catalyst, by using the pulse technique of O_2 and N_2O.

Taking into account the above results and the transient experimental data, a suitable reaction mechanism may be expressed :

$$N_2O\,(g)+S \xrightarrow{\;k_1\;} O \cdot S \tag{6}$$

$$2O \cdot S \underset{k_2'}{\overset{k_2}{\rightleftharpoons}} O_2 \tag{7}$$

$$O_2\,(g)+S \xrightarrow{\;k_3\;} O_2 \cdot S \tag{8}$$

$$CO\,(g)+O_2 \xrightarrow{\;k_4\;} CO_2 \cdot O \cdot S \tag{9}$$

$$CO_2 \cdot O \cdot S \underset{k_5'}{\overset{k_5}{\rightleftharpoons}} CO_2\,(g)+O \cdot S \tag{10}$$

Equations (6), (7), (9) and (10) are for the N_2O–CO reaction and Equations (7),

(8), (9) and (10) are for the O_2–CO reaction.

3-2. Discrimination of Rival Kinetic Parameter-sets

Since the values of k_1 and k_4 were already estimated to be 6.7×10^{-6} and 9.6×10^{-5} mol/g-Ag·min·atm., respectively, five parameters, k_2, k_2', k_3, k_5 and k_5' should be estimated by a parameter optimization technique, using a digital computer. In this estimation, considering many rate constant-sets giving the same degree of fitting to one particular transient data might create difficulties. To minimize this possibility, it is necessary to cross check the rate constant-sets estimated by employing many transient data of the two reactions.

On the N_2O–CO reaction, four kinetic parameters, k_1, k_2, k_2', k_5 and k_5' are unknown. Using the N_2O (inc., 0)–CO_2 response curve in Fig. 6, the best six parameter-sets with the same degree of fitting to the curve are evaluated and they are presented in Table 2 by Sets 1–6. Comparison of the degree of fitting to other transient and steady state rate data is powerful in selecting the best one of the six parameter-sets. The CO–CO_2, O_2–CO_2, CO–N_2, N_2O–N_2 and N_2O–CO_2 responses of the two reactions can effectively be used for this purpose, because the sensitivity of the mode of their response curves depends upon the values of kinetic parameters.[4] Typical results for this search are shown in Fig. 9. The serious regulation is thus carried out for the parameter-sets and Set 6 is concluded to be the best one. Set 6 consistently explains all of the obtained data (see Figs. 6, 15 and 16), and is also in good agreement with the steady state rate data as seen in Fig. 1.

On the O_2–CO reaction, only k_3 is unknown if the kinetic parameters estimated in the N_2O–CO reaction can directly be used. The best value of k_3 is evaluated so as to agree with the steady state data, regardless of the difference of the mode of their transient curves. For this purpose, the CO, O_2 (inc., 0)–CO_2 response on a reduced surface is used as shown in Fig. 10. The value obtained thus is presented in Set 7 in Table 2. Figs. 11 and 12 indicate a good agreement of the calculated steady state rates with the experimental values. Set 7, however, gave a slight overshoot mode for the CO–CO_2 response curves in contrast with

Table 2. Kinetic Parameters Best Fitting the Transient Response Curves

Set No.	$10^5 \times k_1$	$10^6 \times k_2$	$10^4 \times k_2'$	$10^5 \times k_3$	$10^4 \times k_4$	$10^2 \times k_5$	$10^2 \times k_5'$
1	0.67	1.26	10.0	—	0.96	0.10	0.889
2	0.67	0.667	5.0	—	0.96	0.10	0.925
3	0.67	0.019	1.0	—	0.96	0.10	1.11
4	0.67	0.102	0.5	—	0.96	0.10	1.31
5	0.67	0.204	1.0	—	0.96	0.10	0.864
6	0.67	0.148	0.5	—	0.96	0.10	1.17
7	—	0.148	0.5	0.64	0.96	0.10	1.17
8	—	0.148	50.0	50.0	0.96	0.10	1.17

	P_{CO}^o	$P_{N_2O}^o$	P_{He}^o
A	0.05	0.203	0.747
B	0.20	0.203	0.547

(atm)
T = 20°C

● CO_2 } Experimental
○ N_2

—— CO_2 } Calculated
- - - N_2

Fig. 9. The CO-CO_2 and -N_2 responses.

	P_{CO}^o	$P_{O_2}^o$	P_{He}^o
A	0.08	0.200	—
B	—	—	1.00

(atm)
T = 20°C

—— Calculated by Set 7 in Table 2
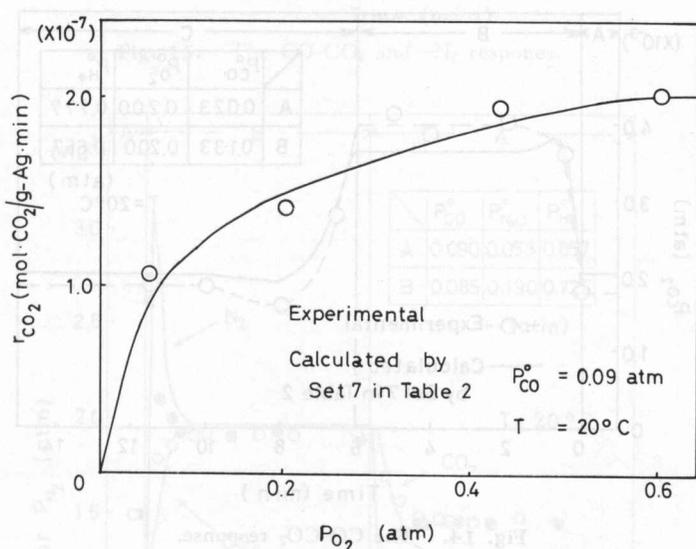○ Experimental
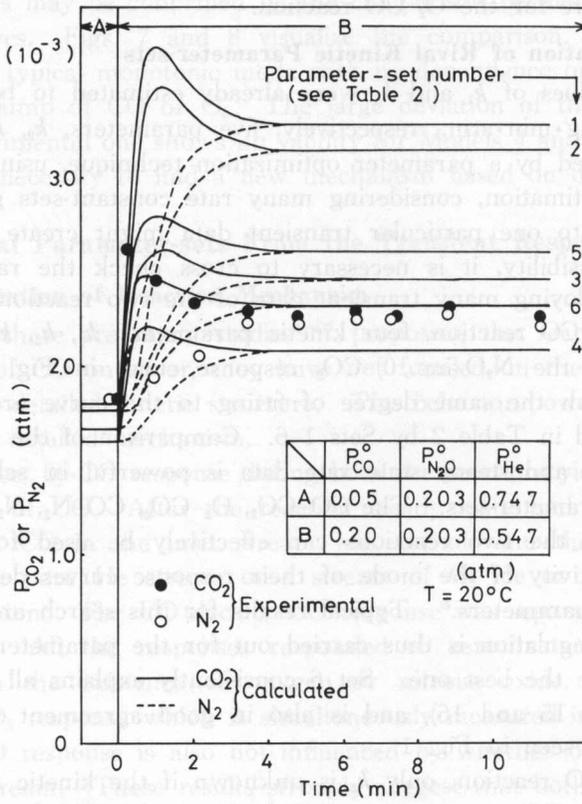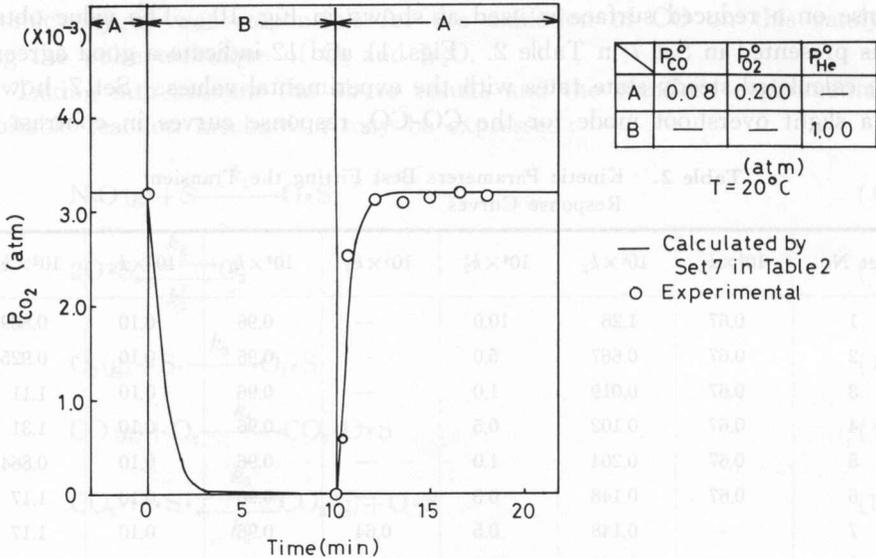
Fig. 10. The CO, O_2(inc., 0)-CO_2 response.
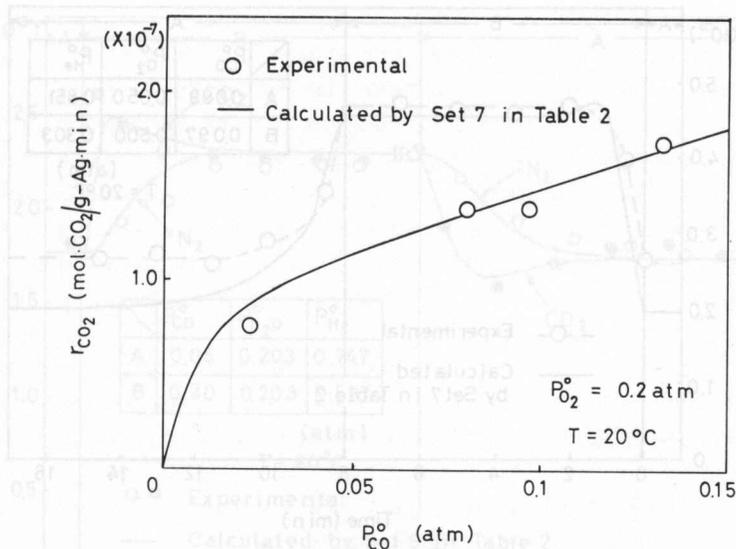
Fig. 11. Plot of r_{CO} vs. P_{CO}.

Fig. 12. Plot of r_{CO_2} vs. P_{O_2}.

the monotonic mode of the experimental $CO-CO_2$ response curves, as can be seen from Figs. 13 and 14. This disagreement strongly suggests a possibility that some kinetic parameters estimated from the N_2O-CO reaction might not be sound for the O_2-CO reaction. In reference 12 it has been discussed that silver surface is heterogeneous for the adsorption of oxygen : all the active sites are not available for the decomposition of N_2O. The most probable possibility may be that k_2 (rate constant for monoatomic oxygen recombination) and/or k_2' (rate constant for diatomic oxygen dissociation) are different between each reaction.
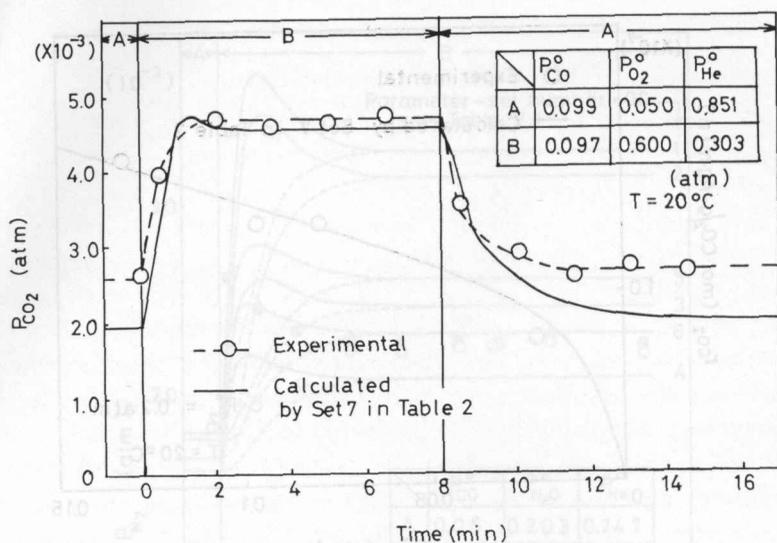
Fig. 13. The O_2–CO_2 response.
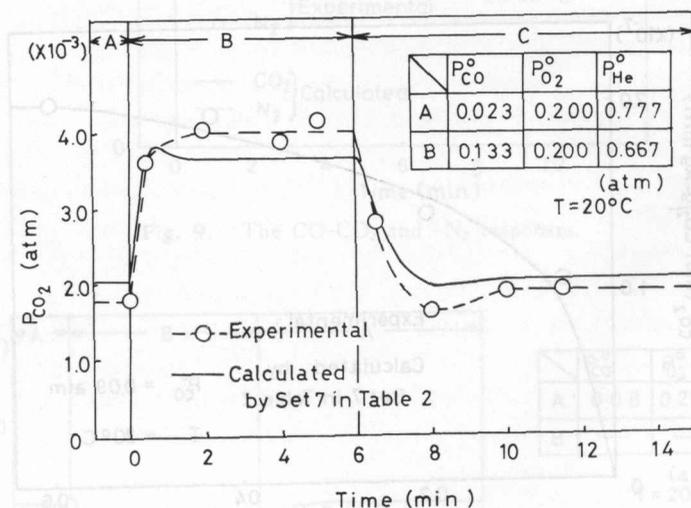
Fig. 14. The CO–CO_2 response.

Consequently, the parameter optimization technique is again applied for evaluating the values of k_2, k_3 and k_2' using a particular CO (inc., 0)–CO_2 response curve. The conclusive values obtained are presented in Table 2 by parameter-set 8. Set 8 consistently explained all other transient response curves, as presented in Figs. 7 and 8 by broken line, providing a good agreement with the steady state rate data as seen in Fig. 2. Comparing Sets 6 and 8 in Table 2, the value of k_2' in the O_2–CO reaction is one hundred times larger than that in the N_2O–CO reaction. This means that adsorbed oxygen in the O_2–CO reaction is very quickly dissociated into monoatomic oxygen rather than the case in the N_2O–CO reac-
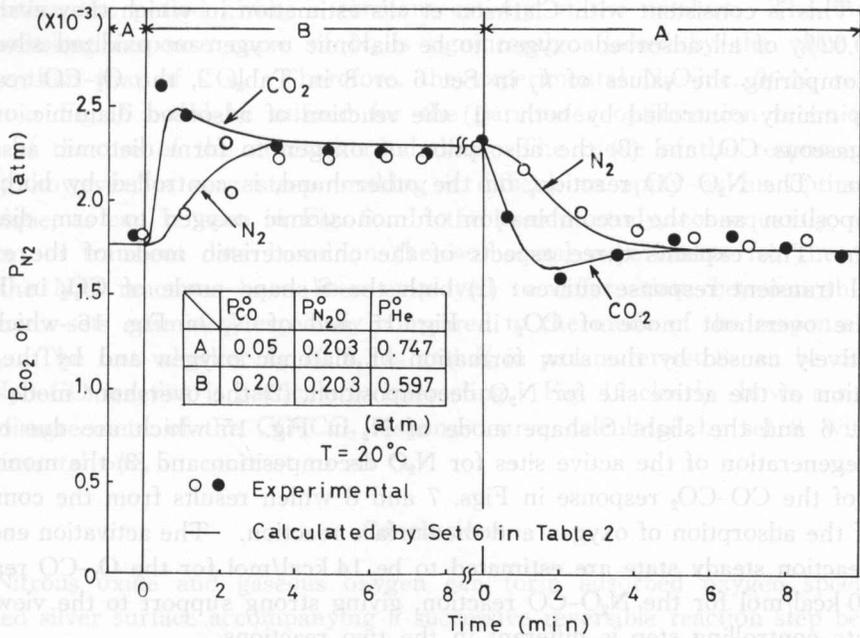
	P_{CO}°	$P_{N_2O}^{\circ}$	P_{He}°
A	0.05	0.203	0.747
B	0.20	0.203	0.597

(atm)

T = 20°C

○ ● Experimental

——— Calculated by Set 6 in Table 2

Fig. 15. The CO–CO_2 and –N_2 respones.

	P_{CO}°	$P_{N_2O}^{\circ}$	P_{He}°
A	0.090	0.053	0.857
B	0.085	0.190	0.725

(atm)
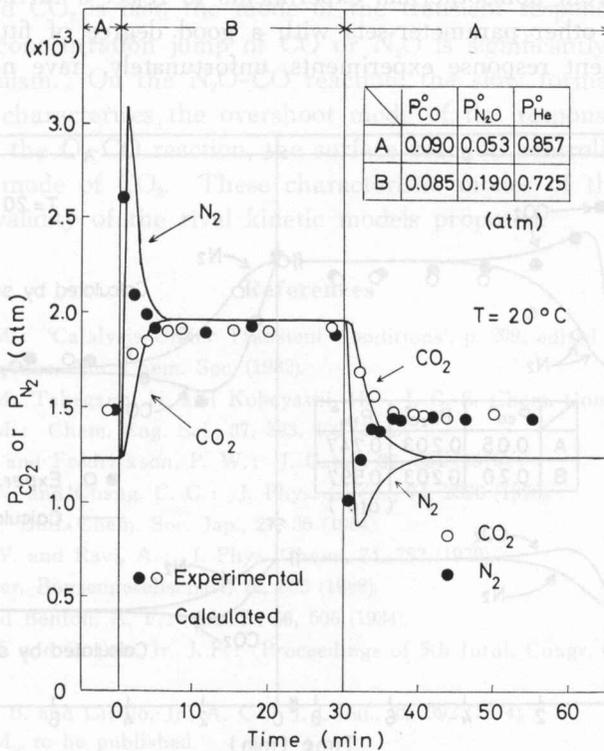
T = 20°C

● ○ Experimental

——— Calculated

Fig. 16. The N_2O–CO_2 and –N_2 responses.

tion. This is consistent with Clarkson et al's estimation in which they evaluated only 0.02% of all adsorbed oxygen to be diatomic oxygen on oxidized silver.

Comparing the values of k_j in Set 6 or 8 in Table 2, the O_2–CO reaction rate is mainly controlled by both : (1) the reaction of adsorbed diatomic oxygen with gaseous CO, and (2) the adsorption of oxygen to form diatomic adsorbed oxygen. The N_2O–CO reaction, on the other hand, is controlled by both N_2O decomposition and the recombination of monoatomic oxygen to form diatomic oxygen. This explains three aspects of the characteristic mode of the experimental transient response curves : (1) both the S-shape mode of CO_2 in Fig. 6 and the overshoot mode of CO_2 in Fig. 15 and of N_2 in Fig. 16 which are respectively caused by the slow formation of diatomic oxygen and by the slow formation of the active site for N_2O decomposition, (2) the overshoot mode of N_2 in Fig. 6 and the slight S-shape mode of N_2 in Fig. 15 which are due to the slow regeneration of the active sites for N_2O decomposition and (3) the monotonic mode of the CO–CO_2 response in Figs. 7 and 8 which results from the combination of the adsorption of oxygen and the surface reaction. The activation energies at a reaction steady state are estimated to be 14 kcal/mol for the O_2–CO reaction and 10 kcal/mol for the N_2O–CO reaction, giving strong support to the view that the rate controlling step is different in the two reactions.

The validity of parameter sets 6 and 8 should additionally be confirmed by using the data from nonisothermal experiments to reject a further possibility of the existence of other parameter-sets with a good degree of fitting. The non-isothermal transient response experiments, unfortunately, have not been carried
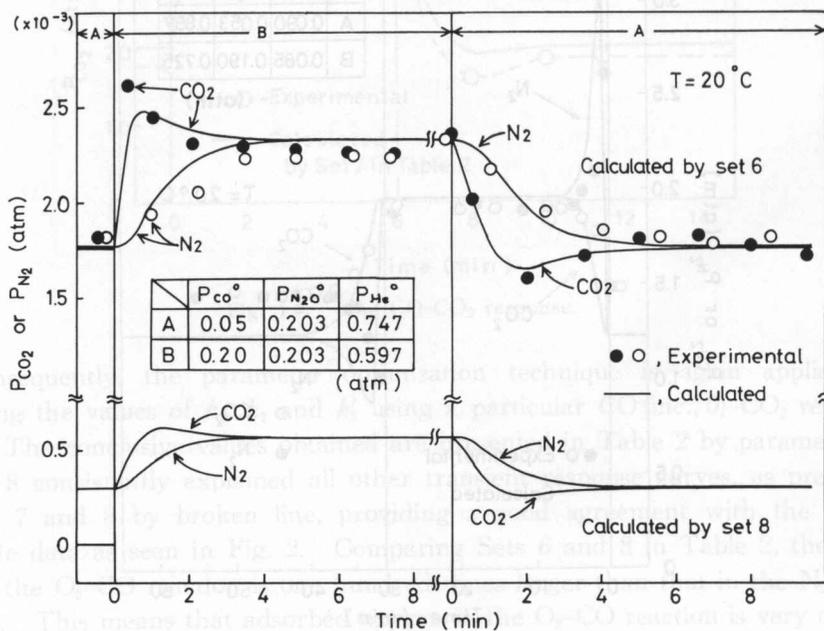

Fig. 17. The CO–CO_2 and –N_2 responses.

out within the period giving a constant activity of the catalyst. The mode of the transient response curve of N_2 is significantly affected by the value of k_j, rather than that of CO_2. Therefore, the experimental $N_2O(\text{inc.}, 0)$–N_2 response curve in Fig. 6 could be utilized for the parameter optimization technique, in stead of the use of the nonisothermal data. The mode of the response curve of N_2, however, is very steep, making it difficult to apply as an optimization technique, as can be seen in Fig. 6. In the present study, consequently, a large number of transient data based on the isothermal experiments for the O_2–CO and the N_2O reactions have been employed to differentiate between the rival parameter-sets estimated, especially compared to the mode of the response curve of N_2. The test whether k_2, k_2', k_4, k_5 and k_5' in parameter-set 8 can be used for the N_2O–CO reaction is particularly interesting. Fig. 17 clearly shows a remarkable disagreement of the CO–CO_2 response curve calculated by set 8 with the experimental one, in contrast to set 6.

Conclusions

Nitrous oxide and gaseous oxygen can form adsorbed oxygen species on reduced silver surface accompanying a successive reversible reaction step between monoatomic and diatomic oxygen. In the course of this sequence, the active oxygen species formed reacts with gaseous CO to produce CO_2. Since the desorption of produced CO_2 is fast, the mode of the transient response curves of CO_2 caused by the concentration jump of CO or N_2O is significantly affected by the reaction mechanism. On the N_2O–CO reaction, the slow formation of diatomic oxygen species characterizes the overshoot mode of the response curves of CO_2 and N_2, and on the O_2–CO reaction, the surface reaction controlling characterizes the monotonic mode of CO_2. These characteristic modes of the curves clearly determine the validity of the rival kinetic models proposed.

References

1) Kobayashi, M.: 'Catalysis Under Transient Conditions', p. 209, edited by A. T. Bell and L. L. Hegedus, Am. Chem. Soc. (1982).

2) Kobayashi, M., Takegami, H. and Kobayashi, H.: J. C. S. Chem. Comm., 37 (1977).

3) Kobayashi, M.: Chem. Eng. Sci., **37**, 393, 403 (1982).

4) Cant, N. W. and Fredrickson, P. W.: J. Catal., **37**, 531 (1975).

5) Keulks, G. W. and Chang, C. C.: J. Phys. Chem., **74**, 2590 (1970).

6) Yamada, N.: Bull. Chem. Soc. Jap., **27**, 36 (1954).

7) Keulks, G. W. and Ravi, A.: J. Phys. Chem., **74**, 783 (1970).

8) Imre, L.: Ber. Bunsengesellschaft, **72**, 863 (1968).

9) Drake, L. and Benton, A. F.: JACS., **56**, 506 (1934).

10) Keulks, G. W. and Outlaw, Jr., J. F.: Proceedings of 5th Intnl. Congr. Catal., Amsterdam (1972).

11) Clarkson, R. B. and Cirillo, Jr., A. C.: J. Catal., **33**, 392 (1974).

12) Kobayashi, M., to be published.